J Mater Sci (2007) 42:1757–1764
DOI 10.1007/s10853-006-0650-2

Mechanical response of nanocrystalline steel obtained by mechanical attrition

R. Rodríguez-Baracaldo · J. A. Benito · J. M. Cabrera · J. M. Prado

Received: 30 May 2006 / Accepted: 6 July 2006 / Published online: 21 December 2006

Abstract The mechanical properties of bulk specimens of nanocrystalline 0.55% C steel with a grain size of 30 nm and a relative density higher than 97% have been determined. Samples were obtained by cold compaction and warm sintering at 425 °C of nanocrystalline powders obtained by mechanical attrition in a planetary ball mill. In both processes an Ar protective atmosphere was used in order to avoid oxygen contamination. X-ray diffraction (XRD) and Transmission electron microscopy (TEM) analysis indicated that a volume-averaged grain size of 30 nm is maintained after the warm consolidation processes. TEM studies also showed equiaxed ferrite with no dislocations inside the grains. However, the grain size distribution was no homogeneous as large grains of 100 nm were observed. An average hardness of 8.5 GPa was obtained, in good agreement with other bulk specimens of nanocrystalline Fe or eutectoid carbon steel prepared by other authors. Compression tests of bulk specimens at a strain rate of $10^{-4}\,s^{-1}$ showed a compression strength near 2,500 MPa with an absolute lack of ductility. Nanoindentation measurements at room temperature provided a strain rate sensitivity parameter of 0.012, indicating that the deformation mechanism is somehow governed by diffusion mechanisms.

R. Rodríguez-Baracaldo
Departament of Engineering, Universidad Nacional de Colombia, Campus la Nubia, Manizales, Colombia

J. A. Benito (✉)
Department of Materials Science and Metallurgy, EUETIB, Technical University of Catalonia (UPC), Comte d'Urgell 187, 08036 Barcelona, Spain
e-mail: Josep.a.benito@upc.edu

J. A. Benito · J. M. Cabrera · J. M. Prado
Centre Tecnològic de Manresa, CTM, Av. Bases de Manresa 1, 08240 Manresa, Spain

R. Rodríguez-Baracaldo · J. M. Cabrera · J. M. Prado
Department of Materials Science and Metallurgy, ETSEIB, Technical University of Catalonia (UPC), vvAv. Diagonal 647, 08028 Barcelona, Spain

Introduction

Nanostructured materials with grain sizes below 100 nm and Ultrafine Grained materials with grain sizes above 100 nm but still in the nanometric range are being actively studied due to the potential mechanical characteristics they could offer [1–3]. Both materials exhibit an enhanced mechanical resistance and hardness in comparison with micrometric grained materials [4, 5]. However, their ductility and toughness are drastically low, a fact that limit the applications of these new materials [4–6].

Recently, the plastic response of nanostructured and Ultrafine Grained materials have been investigated under tensile and compression tests [4, 7–9] and some efforts have been addressed to improve the ductility of these materials [10]. Beside this fact, there is still controversy in the literature upon which is the controlling deformation mechanism. Some authors [11, 12] point out to dislocation glide mechanisms, while other authors [13, 14] suggest Grain Boundary diffusion processes or even mixture models [15]. One of the useful parameters to understand the deformation

kinetics in the nanostructured regime is the strain rate sensitivity parameter of the yield stress. Dislocation glide mechanisms are assumed to be not strain rate sensitive whereas grain boundary diffusion mechanisms are time-dependent.

The scarce experimental data found on the literature about the strain rate sensitivity parameter are characterized by a great scatter, specially for nanostructured metals. This make difficult to check the accuracy of the different models proposed. Although there are few data reported for FCC materials in the range below 100 nm [7, 16, 17], it seems clear that the strain rate sensitivity parameter increases as the grain size decreases. For BCC materials, such as α-Fe, a data compilation is found in the work of Wei et al. [18]. In this study a diminution of the strain rate sensitivity parameter is found from coarse-grained iron to nanosized grains to the extent of being very low strain-rate sensitive at grain sizes around 80–200 nm. However, below 80 nm two trends are encountered. On the one hand, as reported by Koch et al. [19], very low values keeping the decreasing tendency from micrometric grain sizes. On the other hand, an increasing behaviour of the strain rate sensitivity parameter as the grain size decreased below 80 nm as reported by Jang et al. [13]. This disagreement in experimental data is an obstacle in order to determine the role of the deformation mechanisms in nanocrystalline iron.

One of the troubles involved in the determination of mechanical properties in nanostructured materials is the difficulty to obtain specimens large enough to perform conventional test and therefore to characterize the bulk material instead of a nanosection of it. Experimental techniques such as equal channel angular extrusion are very promising in obtaining large samples but unfortunately they have not succeed in producing nanostructured metals, although there is a continuous progress [20]. Up to now the most usual way to get relatively large samples of nanostructured metals is the mechanical milling of powder and subsequent consolidation steps. However, there are some problems associated with this procedure, namely, contamination [21, 22], imperfect particle bonding and volume flaws [4, 23], which adversely influence the measured properties. This is particularly true in explaining the low ductility observed in these samples and the large scatter found in compressive strength or hardness values.

The difficulty in producing bulk nanocrystalline specimens of iron and the difficulty to obtain plastic deformation due to the inherent characteristics of the consolidation techniques explain the few experimental data reported in this metal, specially in a topic as the strain rate sensitivity parameter. In this sense, nanoindentation techniques have been recently used [2, 13,17, 24] to derive the latter parameter. This technique affects a small volume of the sample so most of the problems associated with nanostructured materials obtained from milled powder can be neglected, e.g. porosities and particle bonding. It is expected that nanoindentation techniques could help in provide experimental data that help to understand the mechanical behaviour of nanostructured materials.

Following the data reported in literature, the aim of this work is to establish a consolidation procedure for mechanical milled iron powder to produce bulk specimens of medium carbon steel with a ferritic grain size clearly below 50 nm. The determination of mechanical properties by hardness and compression test as well as the obtainment of the strain rate sensitivity parameter by nanoindentation techniques can make a contribution to understand the controlling deformation mechanism and therefore to improve the ductility of these materials.

Experimental procedure

Iron powder of high purity, with irregular morphology and initial particle size ranging between 75 and 160 μm, was severely deformed in a planetary ball milling for 52 h at a rotating speed of 160 rpm. Stainless steel recipients and Cr-steel balls with 10 mm diameter were used for this purpose. The ratio balls-powder was 27:1. Additionaly a small amount (0.8% weight) of Etilen-bis-stearamide (EBS) was added to avoid the adherence of the powder to the walls of recipient. A light Ar pressure was introduced in the recipients to prevent oxidation during milling. The milling cycle consisted of 30 min of attrition followed by 30 min of stand-by periods in order to minimize the increment of temperature inside the recipient. The final chemical composition in weight percent of the milled powder was 0.55% C, 0.73% O, 0.25% Cr and 0.15% Ni (Fe balance). Due to the high levels of C found, the material was considered as a medium carbon steel powder rather than a pure iron one. The hardness of milled powder was evaluated by Vickers indentations with a load of 0.1 N. Microstructural characterization was performed by Scanning electron microscopy (SEM).

In order to derive the ferritic grain size, X-ray diffraction of the milled powder and consolidated samples was performed in a Siemens equipment using CuKα radiation with wavelength $\lambda = 0.1506$ nm. The instrumental profile was previously determined by

measuring an LaB_6 powder specimen. The correction of $K_{\alpha 2}$ was done using the FULLPROF software [25]. For every diffraction peak, the integral breadth $\beta(d^*)$ was calculated after removal of instrumental broadening. A volume-averaged grain size $<L_v>$ was determined using a modified Williamson–Hall method (Eq. 1), in order to minimize the strain anisotropy caused by line defects [26–28].

$$\beta(d*) = \frac{1}{\langle L_V \rangle} + k(d*)(\rho \bar{C}_{hkl})^{1/2}. \quad (1)$$

Here ρ is the dislocation density and k is a constant depending on the burgers vector **b** and on the effective outer cut-off radius of the dislocations. The values for the average contrast factor $\bar{C}_{hkl}$ for every reflection has been taken from the works of Ungar et al. [29].

Transmission electron microscopy (TEM) analysis of the consolidated samples were carried out in a Philips CM30 microscope operating at 300 kV. After a mechanical grinding to 0.04 mm width, the specimen was ion milled to perforation using a Gatan Duo-mill Model 600 with a liquid-nitrogen cold stage in order to prevent heating. When possible, the grain size was also measured combining bright and dark field images. This procedure allowed to identify the contour of grains free from overlapping effects. Selected area diffraction (SAD) were obtained in all cases.

Fabrication of bulk specimens was done on an INSTRON 8501 testing machine. For this purpose 2.5 g of milled powder was introduced in a cylindrical mould of maraging steel with 9.2 mm of inner diameter. The powder was first compacted at 1,100 MPa for 30 min at room temperature and subsequently heated to 425 °C during 30 min. A slow heating rate was used to prevent thermal gradients in the samples [8]. When the temperature was reached, a pressure of 850 MPa was applied for 60 min. An Ar atmosphere was maintained inside the furnace all along the hot compaction process to prevent oxidation of the specimens. The dimensions of the cylindrical specimens were 5.1 mm in length and 9.2 in diameter. For nanoindentation measurements the same procedure was used, but only with 1.0 g of milled powder, which resulted in a shorter cylinders of 1.9 mm in length and 9.2 mm in diameter.

The hardness of consolidated samples was evaluated by Vickers indentations on the upper and lower flat surfaces of the cylinders applying a load of 1.96 N. At least 15 measures were done for each specimen. The density of samples were determined measuring their dimensions and weight. A value of relative density was calculated taking the theoretical density for iron of 7.87 g/cm^3. The samples were measured several times and the total error calculated was under ±1% of the relative density. No surface open pores were detected so when the samples were weighted in air and water using the Archimedes principle negligible differences were observed between the two methods used.

Compression tests were performed on an INSTRON 8501 testing machine at a quasi-static strain rate of 1×10^{-4} s^{-1}. Teflon sheet and lithium grease was applied in order to minimize friction.

The determination of the strain rate sensitivity parameter was performed using a Nanoindenter XP (MTS) fitted with a *Berkovich* diamond tip. The flat surfaces of the shorter cylinders were carefully polished with alumina until a final size of 0.25 μm. Measurements were performed using the Continuous Stiffness Measurement operation mode, controlling the AC load to give a 2 nm harmonic displacement amplitude at 45 Hz. The samples were allowed to thermally equilibrate with the instrument until the drift rate was measured to be below 0.050 nm/s.

The indentation strain rate was varied from 3×10^{-3} to 10^{-1} s^{-1}. Hardness was averaged over 15 indentations for each strain rate value. The strain rate sensitivity parameter m was determined according to (2):

$$m = \frac{\partial \log H}{\partial \log \dot{\varepsilon}}, \quad (2)$$

where H is the hardness in GPa and $\dot{\varepsilon}$ the strain rate (s^{-1}). Indentations were inspected by SEM in order to verify the absence of cracks.

Results

The morphology of the 52 h milled powder is shown in Fig. 1. At this stage the powder shows an equiaxial shape with a mean particle size of 17 μm. The hardness obtained is 9.3 ± 0.7 GPa and the mean ferritic grain size calculated from XRD is 12 ± 4 nm. Table 1 shows the main characteristics of the cylindrical consolidated samples. The average grain sizes obtained by XRD and TEM micrographs are both very close to 30 nm.

Figure 2 shows bright field and dark field TEM images of consolidated samples in which it is difficult to distinguish between different ferrite grains. The dark field images are particularly useful since they can identify isolated grains [18, 22, 30]. Because some grain overlapping can occurs, specially at very small sizes, this method tend to underestimate the real grain size. The corresponding grain size distribution obtained is

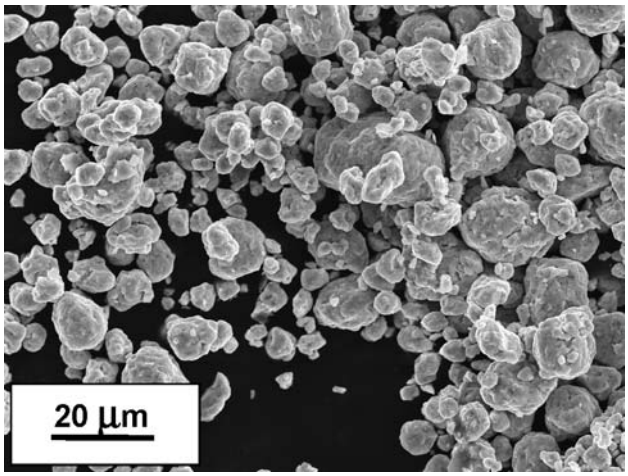

Fig. 1 SEM micrograph showing the morphology and particle size of the iron powder after 52 hours of milling

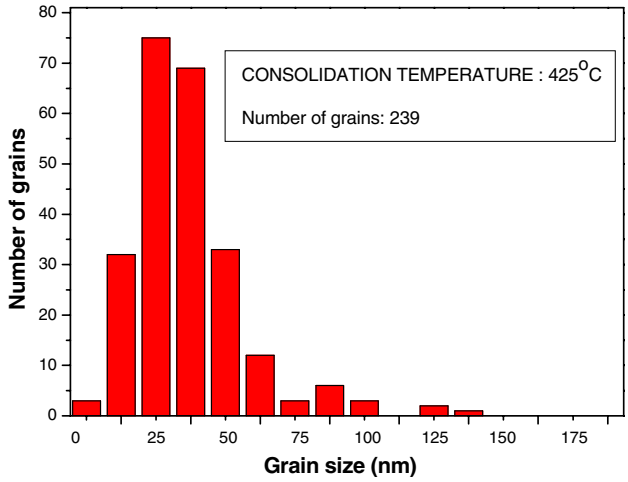

Fig. 3 Grain size distribution in the samples consolidated at 425 °C. The histogram has been determined from TEM micrographs

Table 1 Characteristics of the consolidated specimens

HV (GPa)	% Relative density 5.1 mm × Ø 9.2 mm	% Relative density 1.8 mm × Ø 9.2 mm	Grain size by DRX (nm)	Grain size by TEM (nm)
8.5 ± 0.3	>97%	>97%	28 ± 4	30 ± 19

shown in Fig. 3. Usually, the analysis of grain size distributions of heat treated nanostructured materials displays isolated grains which have grown above the normal distribution [5, 30, 31]. This has also happened in the present case, since several grains with a size above 100 nm have been identified, see Fig. 4. The vast majority of grains studied have an equiaxed shape with large misorientations with neighbouring grains. It must be noted that no evidence of dislocations was found within the ferrite grains. This can be explained by the warm sintering temperature (425 °C), which has probably promoted the partial annealing of ferrite.

The continuous diffraction rings of ferrite in the SAD of Figs. 2 and 4 confirm a random orientation of grains. In highly deformed structures of nanocrystalline iron produced by mechanical attrition [32] or equal channel angular extrusion [20], the diffraction rings tend to be discontinuous. This is due to the alignment of the elongated grains in certain orientations, giving rise to a textured material. The interior of rings corresponding to planes {110} appears usually free of dots, indicating a relatively small presence of oxides or cementite in the samples. Recent studies [33] reported that carbon atoms in mechanically milled pearlitic steel are totally dissolved in ferrite. At similar temperatures than those used in the present study (400 °C), these carbon atoms would be rejected from ferrite grains and segregated into the grain boundaries, promoting

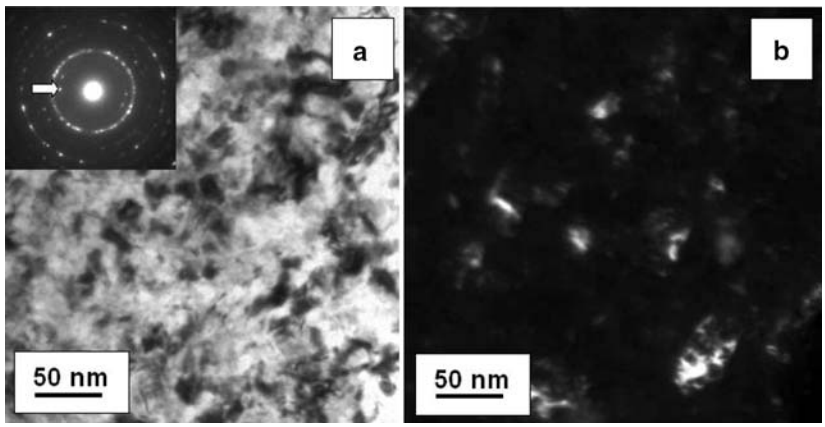

Fig. 2 Bright field (**a**), Dark field (**b**) image and selected-area diffraction (*SAD*) of consolidated samples. The determination of the grain size is difficult even in the dark field image. The *arrow* in SAD shows some spots due to the small presence of cementite precipitation

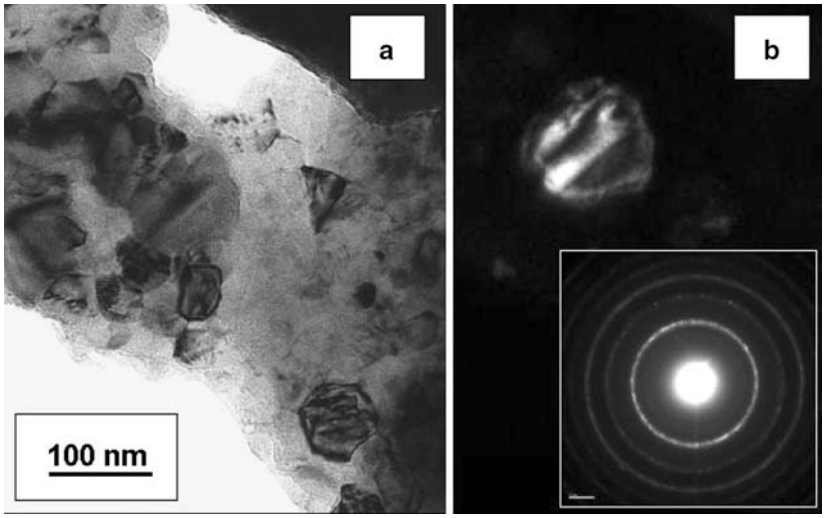

Fig. 4 Bright field (**a**), Dark field (**b**) image and selected-area diffraction (*SAD*) of consolidated samples. In these micrograph isolated grains are clearly visible. A large grain is showed in (**b**), very close to 100 nm grain size. SAD appears free of contamination spots

cementite precipitates. The presence of cementite particles results more evident when the temperature is raised to 475 °C or higher [31, 34]. In the present case, the XRD profile in Fig. 5 shows some diffraction peaks that are attributed to the presence of cementite in the bulk specimens.

The mean hardness value obtained (8.5 GPa) in the consolidated specimens is slightly lower than in the milled powder state. The absolute hardness values [5, 13, 31, 35] and the small diminution of hardness with the treatment at 425 °C agree with others studies of milled pure iron [21, 36], iron with oxide particles [22] or milled steel [37].

The true strain–true stress curve obtained by compression tests at a strain rate of 10^{-4} s^{-1} is shown in Fig. 6. The compressive strength is very close to

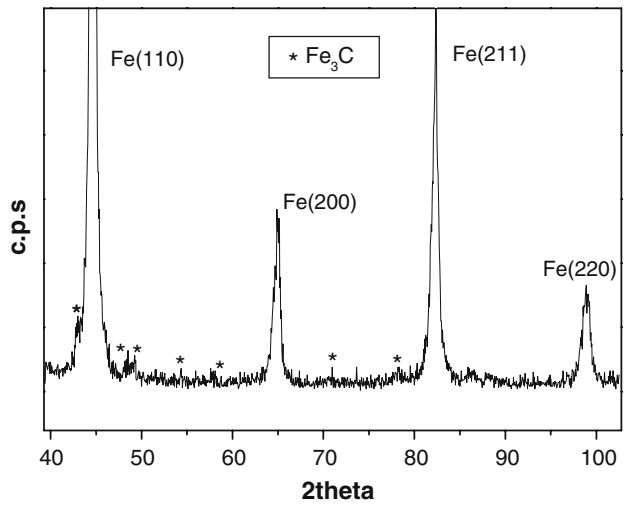

Fig. 5 XRD profile of the consolidated samples after warm sintering at 425 °C. The peaks attributed to cementite are indicated

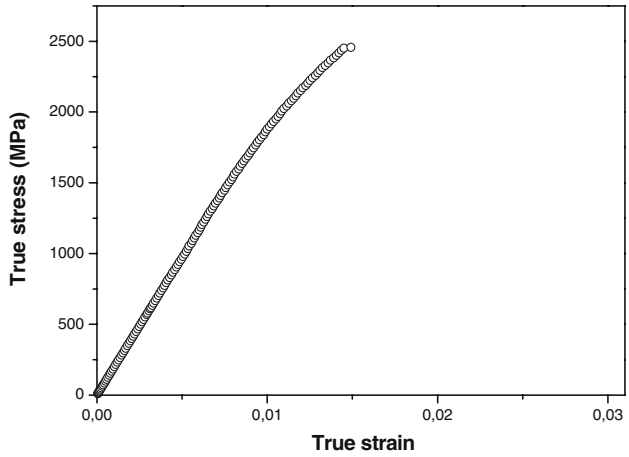

Fig. 6 True stress–true strain standard curve from compression test of consolidated samples. All the samples tested exhibited no plastic deformation

2,500 MPa, with very minor presence of ductility. In any case the strain produced before fracture was greater than 0.018.

The impossibility to calculate the strain rate sensitivity parameter (m) by compression test due to the lack of ductility of the consolidated specimens has been solved by using nanoindentation techniques. The average hardness obtained at each strain rate (from 0.003 to

Table 2 Hardness values of the bulk specimens obtained by nanoindentation at different strain rates

Strain rate (s^{-1})	Hardness (GPa)
0.003	11.05 ± 0.27
0.005	11.15 ± 0.28
0.01	11.23 ± 0.20
0.05	11.42 ± 0.19
0.1	11.55 ± 0.30

0.1 s^{-1}) is listed in Table 2, and plotted in Fig. 7. Data clearly fall in the same trend line showing a strain rate sensitivity parameter of $m = 0.0120 \pm 0.0006$.

Discussion

Compressive strength and ductility

As described before, the 0.55% C steel bulk specimens with a ferritic grain size of 30 nm have a high compressive strength combined with brittle behaviour. This is the common trend reported in the literature in the few available results [4, 8] of mechanical properties of iron or steel with grain size below 50 nm. In the studies of Khan et al. [8, 38], cylindrical samples with 9.4 mm in diameter and a porosity between 3 and 7% were tested at 10^{-4} s^{-1}. The compressive strength found was 2,000 and 1,600 MPa for samples with grain size of 36 and 50 nm, respectively. In both cases the maximum strain attained was 0.01. The larger compressive strength obtained in the present work (near 2,500 MPa) for a similar grain size can be explained by the lower porosity and the presence of cementite particles.

The lack of ductility in nanocrystalline ferrite with grain size below 50 nm was also studied by Koch et al. [4] with small disks of 3.18 mm in diameter and 0.5 mm in height obtained by warm consolidation. Their samples had a grain size between 8 and 33 nm and were tested in biaxial tension. All samples showed brittle behaviour and SEM inspection demonstrated the presence of debonding between the original particles of the milled powder. Only when the zones of incomplete bonding decreased in size, an increase in strength was noticed.

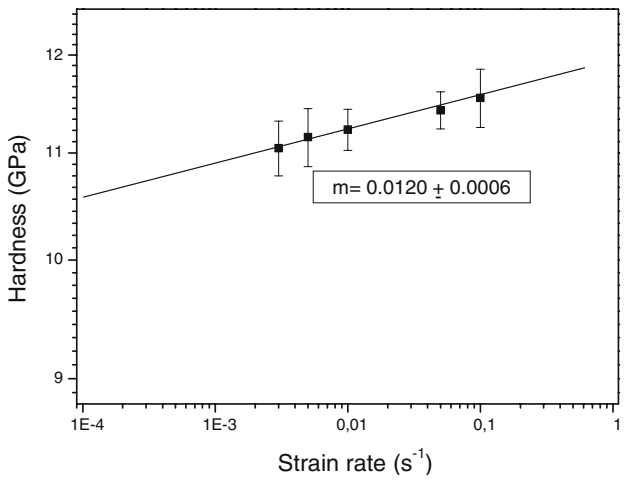

Fig. 7 Hardness as a function of the indentation strain rate. Each point in the plot represents the average of at least 15 measures

Plastic deformation in nanocrystalline iron and steel has been described [5, 8, 20, 31] for bulk specimens with grain size greater than 50 nm and smaller than ~300 nm. Bulk nanocrystalline iron specimens with grain size above 80 nm obtained by mechanical milling [5, 8] and Equal Chanel Angular Extrusion [20] showed plastic deformation during compression tests, being shear banding the predominant plastic deformation mechanism. It is worth noting that in the case of the bulk specimens obtained from milled iron, almost full density specimens were obtained after long consolidation processes. However, Zhang et al. [31] have shown that some plastic deformation (6%) without shear banding can be achieved in an eutectoid steel produced by spark plasma sintering with an average grain size of 57 nm and only 89% of relative density. This plastic behaviour seems to be related to a good metallurgical bonding between particles due to the removal of oxides or impurities in the surface of powder particles. The absence of shear banding could be also explained by the cementite precipitates inside the grain and along the grain boundaries.

In the present work, no signs of microscopic plastic deformation was observed after SEM inspection of the fracture surfaces. This fact could be explained by the small ferrite grain size of the present case, well below 50 nm. Moreover, partial debonding between former powder particles and presence of volume flaws due to the porosity can lead to fracture before the material can show any microscopic ductility. Finally, the presence of cementite due to contamination during milling could lead to inactivation of shear band formation.

Strain rate sensitivity

As explained in the introduction, the reported behaviour of the strain rate sensitivity parameter m in BCC iron when the grain size is well below 100 nm is not clear. At this point it is interesting to note that Ma et al. [5] have reported in near full density samples of iron a constant diminution of m from 0.04 in the microcrystalline range to 0.0049 in the nanocrystalline one (80 nm). Furthermore, in the work of Wei et al. [18] about the variation of m with grain size in BCC metals, an increase of m is not expected to occur at grain sizes smaller than 80 nm. In accordance with this tendency, very low values of m have been reported in the work of Koch et al. [19]. In that work, the parameter m was obtained by an automated ball indentation technique on warm compacted bulk specimens. They found that m varied between –0.0038 and

0.0067 within the 15–24 nm range. However, Jang et al. [13] have reported larger values of m when the grain size is smaller than 50 nm. In that work, increasing parameter m is found at decreasing grain size (from $m = 0.006$ in samples with macroscopic grain size to $m = 0.025$ when the grain size was 10 nm).

The value of $m = 0.0120 \pm 0.0006$ found here for a grain size of 30 nm fits better with the tendency exposed in the studies of Jang et al. than that observed by Koch et al. The possible reasons for this disagreement in the values of m are summarized as follows. One reason could be the role played by porosity and bonding between the former powder particles in the bulk specimens. For instance, in the studies of Jang et al. [13], the bulk specimens were obtained by cold compaction without any warm consolidation step. A poor metallurgical bonding must then be expected in those samples. They minimized the role of the interparticle zones by the combination of a great particle size with a small indentation size of the nanoindentation technique used. Therefore, no effect of interparticle sliding was assumed to affect the m values obtained there. On the other hand, in the studies of Koch et al. [19, 35] the indentation size was very large, so a great number of grains and former powder particles were involved in the measures. In the present work the indentation size was also large enough to involve a moderate number of former powder particles. Since the interparticle effects could also be affecting the values both in the studies of Koch et al. and the present one, no relationship can be establish between the interparticle effects and the strain rate sensitivity reported.

The amount of impurities located in the grain boundary would be another point to discuss since impurities are related to the loss of activity of grain boundary sliding mechanism, decreasing the strain rate sensitivity parameter m. In the work of Jang et al. [13] C and O concentrations are unknown. On the contrary, in the work of Koch et al. [35] the level of impurities in the consolidated specimens are ~0.5% for O and below 0.1% for C (weight percent). These impurity levels are lower than in the present material, so grain boundary sliding would be more active in the Koch material than in the present one and therefore a lower value of m would be expected. Since the obtained value of m is higher than in the one reported by Koch et al. [19], the loss of activity of grain boundary sliding mechanism cannot be the reason for the disagreement in the values of m.

The grain boundary relaxation due to the heat treatment in the consolidation procedure has also been suggested to be the possible reason for the low m reported by Koch et al. [20]. However, similar grain boundary relaxation must be occurring in Koch and present results as the consolidation procedure was very similar.

The differences found here between literature results, together with the present one on the m value at grain sizes under 50 nm are important because creates uncertainty about the deformation mechanisms involved in nanocrystalline ferrite. Dislocation glide is assumed to be the dominant mechanism in BCC nanocrystalline ferrite. At these small grain sizes the grain boundaries turns to be the main obstacle to dislocation glide, so the smaller the length between grain boundaries the greater the increment observed in flow stress.

Nevertheless, dislocations slip mechanism are not rate-sensitive and the m values obtained could indicate that a diffusion driven process such as grain boundary (GB) sliding, would be activated [13]. A m of 0.012 seems to be small for diffusion-controlled plastic flow to become predominant since it is believed [7] that a m higher than 0.5 is need. The present low, but significant strain rate sensitivity parameter suggest a mixture model on which both deformation mechanisms would be active in bcc metals as the grain decreases in the nanocrystalline range [14].

Conclusions

Cylindrical 0.55% C steel bulk specimens of 5.1 mm height and 9.2 mm in diameter have been produced by warm consolidation process from milled iron powder. The mean grain size determined by XRD and TEM techniques was 30 nm. Presence of Fe_3C was detected in the samples. The porosity was lower than 3%.

The hardness (8.5 GPa) is in good agreement with the Hall–Petch relationship for iron or milled steel and the compressive strength of 2,500 MPa is slightly above the values found in other studies. Samples failed with almost no plastic deformation. The shear bands mechanism described for ferrite with grain sizes above 50 nm was no detected here. The strain rate sensitivity parameter has been measured by nanoindentation techniques, obtaining a value of 0.012, which could lead to the existence of some activity of diffusion driven deformation mechanism in the nanocrystalline steel apart from the dominant dislocation slip processes.

Acknowledgements The authors wish to thank Drs. Antoni Roca and Jordi Llumà for help in the studies of the milled powder as well as Pep Bassas and Montserrat Marçal for

assistance in XRD and SEM observations, respectively. The authors also thank the assistance provided by Dr. Jaume Caro in the nanoindentation tests. This work was supported by CICYT (project DPI 2005-09324). R. Rodríguez-Baracaldo is also grateful for the Fundación Carolina grant.

References

1. Gleiter H (1989) Prog Mat Sci 33:223
2. Valiev RZ, Alexandrov IV, Zhu YT, Lowe TC (2002) J Mat Res 17:5
3. Rawers J, Krabbe R (1998) J Mat Synth Process 6:133
4. Mallow TR, Koch CC (1998a) Acta Mater 46:6459
5. Jia D, Ramesh KT, Ma E (2003) Acta Mater 51:3495
6. Kim HS, Estrin Y (2001) Appl Phys Lett 79:4115
7. Cheng S, Ma E, Wang YM et al (2005) Acta Mater 53:1521
8. Khan AS, Zhang H, Takacs L (2000) Int J Plast 16:1459
9. Takaki S, Kawasaki K, Futamura Y, Tsuchiyama T (2006) Mater Sci Forum 503–504:317
10. Wang YM, Ma E (2004a) Acta Mater 52:1699
11. Wang YM, Ma E (2004b) Mat Sci Eng A 375:46
12. Asaro RJ, Suresh S (2005) Acta Mater 53:3369
13. Jang D, Atzmon M (2003) J Appl Phys 93:9285
14. Van Swygenhoven H, Caro A (1997) Appl Phys Lett 71:1652
15. Kim HS, Estrin Y (2005) Acta Mater 53:765
16. May J, Höppel HW, Göken M (2005) Scrip Mater 53:189
17. Schweiger R, Moser B, Dao M et al (2003) Acta Mater 51:5159
18. Wei Q, Cheng S, Ramesh KT, Ma E (2004a) Mat Sci Eng A 381:71
19. Mallow TR, Koch CC, Miraglia PQ, Murty KL (1998) Mat Sci Eng A 252:36
20. Wei Q, Kecskes L, Jiao T et al (2004b) Acta Mater 52:1859
21. Mallow TR, Koch CC (1997) Acta Mater 45:2177
22. Kimura Y et al (2000) In: Symposium on ultrafine grained materials at the 2000 TMS annual meeting, Edited by the minerals, metals and materials society, p 277
23. Nieman GW, Weertman JR, Siegel RW (1991) J Mat Res 6:1012
24. Mueller J, Durst K, Amberger D, Göken M (2006) Mat Sci Forum 503–504:31
25. FullProf, Rodríguez Carbajal J (2004) Laboratoire Léon Brillouin (CEA-CNRS). Centre d'etudes de Saclay, 91191, Gif sur Yvette, Cedes, France
26. Williamson GK, Hall WK (1953) Acta Metall 1:22
27. Scardi P, Leoni M, Delhez R (2004) J Appl Cryst 37:381
28. Ungar T, Tichy G (1999) Phys Stat Sol A 171:425
29. Revesz A, Ungar T, Borbely A, Lendvai J (1996) Nanostruct Mater 7:779
30. He L, Ma E (1996) J Mat Res 11:72
31. Zhang HW, Gopalan R, Mukai T, Hono K (2005) Scrip Mater 53:863
32. Murayama M, Howe JM, Hidaka H, Takaki S (2003) ISIJ Int 43:755
33. Ohsaki S, Hono K, Hidaka H, Takaki S (2005) Scrip Mater 52:271
34. Lluma J, Benito JA, Roca A, Cabrera JM, Prado JM (2006) Mat Sci Forum 503–504:1007
35. Mallow TR, Koch CC (1998b) Metall Mater Trans A 29:2285
36. Kim J, Umemoto M, Liu ZG, Tsuchiya K (2001) ISIJ Int 41:1389
37. Xu Y, Umemoto M, Tsuchiya K (2002) Mater Trans 43:2205
38. Khan A (2006) Int J Plast 22:195